Copy No. 9

NASA Program Apollo Working Paper No. 1094

AN EXPERIMENTAL INVESTIGATION OF APOLLO COMMAND MODULE STATIC FLOTATION CHARACTERISTICS

[redacted]

NATIONAL AERONAUTICS AND SPACE ADMINISTRATION

MANNED SPACECRAFT CENTER

Houston, Texas

January 30, 1964

NASA PROGRAM APOLLO WORKING PAPER NO. 1094

AN EXPERIMENTAL INVESTIGATION OF APOLLO COMMAND MODULE STATIC FLOTATION CHARACTERISTICS

Prepared by: RWBuiker

for R. B. Grow
Aerospace Technologist

J. B. Slight

J. B. Slight
Mechanical Engineering Technician

Authorized for Distribution:

Warren Gillespie, Jr.

for Maxime A. Faget
Assistant Director
for Engineering and Development

NATIONAL AERONAUTICS AND SPACE ADMINISTRATION
MANNED SPACECRAFT CENTER
HOUSTON, TEXAS

January 30, 1964

TABLE OF CONTENTS

LIST OF TABLES

LIST OF FIGURES

AN EXPERIMENTAL INVESTIGATION OF APOLLO COMMAND MODULE STATIC FLOTATION CHARACTERISTICS

SUMMARY

A preliminary investigation of the flotation characteristics of the Apollo Command Module was initiated in order to determine any undesirable flotation characteristics prior to "freezing" of the design. One-fifth geometrically scaled models of the proposed Apollo command module (slightly different from the production configuration) were tested in a water tank and necessary data were obtained to yield flotation characteristics. Results showed that a spacecraft of this shape can be designed to have desirable flotation characteristics.

INTRODUCTION

Experience has shown that it is desirable to have, as early as possible in the design stage of a spacecraft, a complete knowledge of the postlanding hydrostatic flotation characteristics to insure mission reliability. Lack of this knowledge in the Mercury Program caused some undesirable flotation characteristics which were not discovered until after the major portion of the design was "frozen" and the spacecraft had reached the developmental stage. As a result, methods had to be devised which would bring the flotation characteristics within acceptable limits. These methods were effective but resulted in a less efficient Mercury spacecraft design.

During a study reported herein, geometrically scaled models of a proposed Apollo command module configuration were tested in water by systematically varying the center of gravity in order to obtain data required to describe the flotation characteristics. The resulting data, in the form of buoyancy force lines, angles of heel, and righting moments, are presented in graphical form.

TEST PROCEDURE

Models

The test program was carried out using two models, one representing the internal pressure vessel and the other representing the external geometry of the command module. This approach was based on the assumption that the outside shape (overall command module configuration) would not be watertight and that actual flotation characteristics would be dictated by the shape of the pressure vessel plus the buoyant effect of the immersed outside structure and material which occupy the space between the two configurations. The models were constructed of fiberglass and geometrically scaled from the proposed full-scale configurations (figs. 1 and 2) to be one-fifth size. The weights of these models were only approximately half their scaled test weights in order that the weights required to bring the models to their true test weights could be used to change the location of the center of gravity. Each model was encircled by two rings which contained holes for the purpose of attaching the desired added weights (figs. 3 and 4).

Since the weight scale factor is the cube of the model geometric scale, or $\frac{1}{125}$ in the case of $\frac{1}{5}$ scale models, and the full scale weights were estimated as 6,517 and 7,500 pounds, the required model scaled weights, were 52.13 and 60.00 pounds, respectively. However, since the tests were to be conducted in fresh water, the above weights were adjusted for sea water conditions by dividing them by the specific gravity of sea water (1.026). The actual test weights for the models were thus 50.82 and 58.48 pounds.

Tests

The first step in performing a test was to establish the center of gravity (c.g.) location of a given model-ring combination and to determine its weight, from which the weight to be added (to obtain the desired total test weight) was easily determined. The added weight was then suspended on a pivot from one of the holes in one of the encircling rings. The point of suspension could be changed in this way to give the effect of stabilizing the model at different angles of heel.

Since the external weight was submerged during a test, compensation was made for the buoyancy force of the water on this weight. The buoyant force effect of the rings was neglected since it was found that the rings had a maximum displacement of less than one percent of the model displacement.

The model and added weight were then placed in a tank of water and allowed to reach a stable attitude. The location of the suspended weight and the points of intersection of the waterline on the ring were recorded for each position at which the model was stabilized. Test data for the two models are presented in tables I through IV. Each of the two models was tested for the two established weight conditions (6,517 and 7,500 pounds full scale).

The tests were made primarily to determine the following:

1. Regions of center of gravity (c.g.) location which would result in basically different spacecraft flotation characteristics.

2. Stable attitudes for any predicted spacecraft postlanding c.g. location.

3. Portions of the spacecraft which would be below the waterline at any given predicted spacecraft attitude.

4. Changes in attitude resulting from movement of astronauts.

RESULTS AND DISCUSSION

Method of Analysis

Full scale drawings of the models and rings were made and spacecraft stations, load application points, and the combined model-ring c.g. location were established on these drawings. Figure 5 is a scale representation of one of these drawings (pressure vessel at 6,517 pounds displacement) and will be used as an example to discuss the method used to determine the buoyancy force lines of action intersection with the vertical centerline, angle of heel, and waterline-centerline intersection stations. A waterline was established on the drawing by connecting points A and B which were recorded during the test phase. This is shown as line AB on figure 5. The waterline-centerline intersection station, point D, was determined by scale measurement from a known station, and the angle of heel of the spacecraft centerline relative to a perpendicular to the surface of the water was measured. The vector produced by the suspended weight was drawn through its attachment point, and the vector produced by the model-ring combination was drawn through the model-ring c.g. These points are labeled C and G respectively on figure 5. Both of these vectors were drawn normal to the waterline and the perpendicular distance between the two, line GF, was measured. Since the test configurations had purposely been assembled in a manner which resulted in a coplaner force system, the analytical summation of moments about point G determined the distance GE. The buoyancy force vector was then drawn through point E normal to the waterline and extended to cross the spacecraft vertical centerline at point M. This force is the equivalent force imposed on the model system by the water and as such acts through the composite c.g. of the complete system. Therefore, with the spacecraft c.g. located at any point on this line, the spacecraft will be stable at this angle of heel. This procedure was repeated for every position at which each model was stabilized during the flotation phase and the results recorded under calculated data in tables I through IV.

These data were then used to plot the angle of heel vs buoyancy force lines of action for each model and each test displacement. This facilitates the location of the buoyancy force line of action intersection with the spacecraft centerline for any angle of heel between 0 and 180 degrees. These curves are shown in figures 6 through 9. Using these curves, drawings were made showing the buoyancy force lines of action and their respective intersection points with the vertical centerline for various angles of heel between 0 and 180 degrees. Scale reproductions of these drawings are shown in figures 10 through 13. Any spacecraft c.g. can be located on these drawings and the righting or upsetting level arm (the perpendicular distance from the buoyancy force vector to the c.g.) can be measured.

Figures 14 and 15 are a result of fairing the buoyancy force lines of action of figures 10 through 13 and from three significant c.g. regions. With the c.g. located in region 1, the spacecraft would be stable at one attitude with an angle of heel between 0 and 90 degrees, dependent upon the location of the c.g. within this region. A c.g. located in region 2 would make the spacecraft stable at one attitude with an angle of heel between 90 and 180 degrees, dependent upon the location of the c.g. within this region. If the c.g. is located in region 3, the spacecraft would be stable at two attitudes. One of these stable attitudes would be at an angle of heel between 0 and 90 degrees and the other would be at an angle of heel between 90 and 180 degrees.

Figures 16 through 18 are plots of the righting movements vs angle of heel for the full scale spacecraft at specified c.g. locations. For example, in making the plot of the pressure vessel curve shown in figure 16, the specified c.g. was located on figure 10. The perpendicular distances from the c.g. to the buoyancy force lines of action shown on the figure were then measured. Each of these moment arms was then multiplied by the spacecraft weight and divided by 12 to give the righting or upsetting moment in foot-pounds. Using these data, and assuming clockwise moments to be negative, a curve can be plotted from 0 to 180 degrees angle of heel. The stable attitudes of the spacecraft can then be determined by noting the angle of heel at which the righting moment curve crosses the zero moment line in a positive direction, in this case, 8.5 and 150 degrees. The spacecraft is also theoretically stable at the point where the righting moment line in a negative direction or in this case, 106 degrees. However, a very small change in attitude would cause the spacecraft to revert to one of the other stable positions. Positive righting moments will decrease the angle of heel, and negative righting moments will increase the angle of heel.

Results

Figures 19 and 20 contain the information necessary to determine what portion of the spacecraft is below the surface of the water. The curves are plots of the calculated data shown under waterline and centerline intersection station of tables I through IV. Angles of heel between 70 and 110 degrees are not shown because they could not be accurately determined during model tests. Furthermore, as the angle of heel approached 90 degrees, the waterline-centerline intersect points approached infinity. (At 90 degrees, the waterline does not intersect the centerline.)

Figures 21 and 22 pictorially illustrate flotation characteristics during astronaut egress. The waterline and angles of heel shown in these figures are based on pressure vessel flotation characteristics only. The spacecraft was assumed to weigh 6,517 pounds and the c.g. to be located at station 109, offset seven inches from the vertical centerline with the astronauts on their couches. With this weight and c.g. location, the spacecraft has two stable positions (fig. 16). Figure 21 illustrated the normal upright stable position and figure 22 the inverted stable position. Illustration (A) in each of these figures shows the stable attitudes of the spacecraft before the astronauts begin egress. Illustration (B) shows the attitudes of the spacecraft with an astronaut sitting on the hatch sill, and (C) shows the attitudes after the astronauts have left the spacecraft.

Once the geometry of a floating body (spacecraft) has been defined, the two major factors which determine its flotation characteristics are its weight and c.g. location. In the Apollo configuration tested, there are three regions of c.g. location which result in significantly different flotation characteristics.

CONCLUDING REMARKS

Since this program was initiated, there have been changes in the Apollo command module geometry which will result in slightly different flotation characteristics. As it is not possible to extrapolate data for the present design from the results obtained from testing the models used in this program, it is recommended that further testing be accomplished, using models of the latest Apollo command module flotation geometry.

TABLE I.- TEST DATA FOR PRESSURE VESSEL
MODEL AT 6,517 POUNDS DISPLACEMENT

Test Data				Calculated Data		
Load Application Pt.		Waterline Intersect Points on Ring		Heel Angle, Degrees	Buoyancy Force and Centerline Intersection Sta. Inc.	Waterline and Centerline Intersection Sta. In.
X, In.	Y, In.	Load Side	Other Side			
1.263	-12.739	267.5°	98.0°	2.75°	63.0	118.00
2.497	-12.554	270.0°	100.0°	5.00°	62.5	117.65
3.716	-12.248	272.0°	103.0°	7.75°	61.3	118.30
4.901	-11.826	274.0°	105.5°	10.00°	60.3	118.60
6.033	-11.288	276.5°	107.5°	11.50°	59.7	119.00
7.112	-10.643	279.0°	110.5°	14.75°	62.0	118.70
8.120	- 9.894	282.0°	114.0°	18.00°	65.0	119.20
9.051	- 9.051	284.5°	117.0°	21.00°	67.8	119.60
9.894	- 8.120	288.0°	121.5°	24.75°	71.6	120.40
10.643	- 7.112	291.0°	126.0°	28.75°	74.8	121.70
11.288	- 6.033	295.5°	132.0°	33.75°	78.0	123.20
11.826	- 4.901	300.5°	136.0°	38.25°	81.2	123.30
12.248	- 3.716	306.0°	146.0°	46.00°	85.8	128.40
12.652	- 2.517	312.5°	155.0°	54.00°	90.0	133.60
13.037	- 1.284	321.0°	168.0°	64.50°	95.2	147.30
13.037	1.284	339.5°	194.0°	87.00°	104.6	--
12.652	2.517	350.0°	208.0°	99.00°	108.8	--
12.248	3.716	0.0°	220.0°	110.00°	112.4	--
11.826	4.901	8.5	230.0°	119.50°	115.0	64.30
11.288	6.033	16.5°	237.5°	127.00°	117.0	73.70
10.643	7.112	23.0°	244.0°	136.50°	119.2	78.40
9.894	8.120	29.0°	249.5°	139.50°	120.0	81.80
9.051	9.051	34.0°	254.0°	144.00°	120.5	84.10
8.120	9.894	39.0°	258.0°	148.75°	121.0	86.20
7.112	10.643	43.5°	262.5°	153.00°	121.2	87.20
6.033	11.288	48.5°	266.0°	157.00°	121.0	88.30
4.901	11.826	52.5°	270.0°	161.25°	120.5	89.60
3.716	12.248	57.0°	274.0°	165.50°	118.5	90.40
2.497	12.554	61.5°	278.0°	170.00°	117.5	90.90
1.263	12.739	66.5°	283.0°	175.00°	118.0	91.30

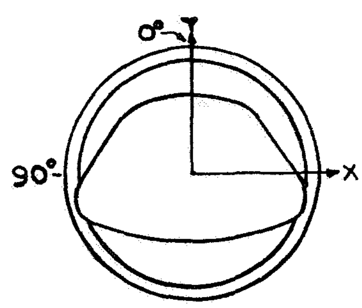

TABLE II.- TEST DATA FOR PRESSURE VESSEL
MODEL AT 7,500 POUNDS DISPLACEMENT

Test Data				Calculated Data		
Load Application Pt.		Waterline Intersect Points on Ring		Heel Angle, Degrees	Buoyancy Force and Centerline Intersection Sta. In.	Waterline and Centerline Intersection Sta. In.
X, In.	Y, In.	Load Side	Other Side			
1.263	-12.739	269.5°	96.25°	2.80°	62.6	115.7
2.497	-12.554	272.0°	99.00°	5.50°	64.5	115.9
3.716	-12.248	274.5°	102.00°	8.25°	65.9	116.2
4.901	-11.826	277.0°	104.50°	11.75°	64.5	116.2
6.033	-11.288	280.0°	107.50°	13.75°	67.2	116.2
7.112	-10.643	282.5°	110.00°	16.25°	65.8	116.2
8.120	- 9.894	286.0°	114.00°	20.00°	70.6	116.7
9.051	- 9.051	289.0°	118.00°	23.50°	72.7	117.5
9.894	- 8.120	293.0°	123.00°	28.00°	77.1	118.5
10.643	- 7.112	297.0°	128.00°	32.50°	79.7	119.3
11.288	- 6.033	302.0°	134.00°	38.00°	83.5	120.8
11.826	- 4.901	307.0°	141.00°	44.00°	86.9	123.3
12.248	- 3.716	313.0°	149.00°	51.00°	90.7	126.9
12.652	- 2.517	319.0°	158.00°	58.50°	94.4	133.0
13.037	- 1.284	326.0°	168.00°	67.00°	97.0	144.8
13.037	1.284	340.5°	190.50	85.50°	102.9	---
12.652	2.517	352.0°	203.00°	97.50°	107.5	-26.0
12.248	3.716	0.5°	214.00°	107.25°	110.6	46.2
11.826	4.901	8.5°	223.50°	116.00°	113.2	65.9
11.288	6.033	16.5°	232.00°	124.25°	115.8	75.5
10.643	7.112	23.0°	239.00°	131.00°	117.3	80.3
9.894	8.120	30.0°	245.00°	137.50°	119.2	84.6
9.051	9.051	35.0°	250.00°	142.50°	119.2	86.3
8.120	9.894	40.5°	255.00°	147.75°	120.4	88.3
7.112	10.643	46.0°	260.00°	153.00°	121.6	89.8
6.033	11.288	50.0°	264.00°	157.00°	120.7	90.4
4.901	11.826	55.0°	268.00°	161.50°	120.7	91.7
3.716	12.248	60.0°	272.00°	166.00°	120.7	92.7
2.497	12.554	64.0°	276.00°	170.00°	119.3	93.0
1.263	12.739	69.0	280.00°	174.50°	118.0	93.7

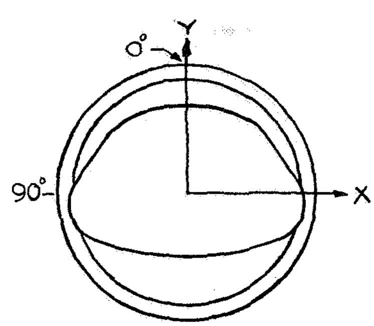

TABLE III.- TEST DATA FOR EXTERNAL
CONFIGURATION AT 6,517 POUNDS DISPLACEMENT

Test Data				Calculated Data		
Load Application Pt.		Waterline Intersect Points on Ring		Heel Angle, Degrees	Buoyancy Force and Centerline Intersection Sta. In.	Waterline and Centerline Intersection Sta. In.
X, In.	Y, In.	Load Side	Other Side			
1.880	-15.890	92.25°	265.25°	1.25°	--	130.7
3.122	-15.693	91.50°	264.50°	2.00°	- 77.7	130.8
4.342	-15.400	90.50°	263.50°	3.00°	- 49.9	130.8
5.538	-15.011	89.75°	262.50°	3.75°	- 51.4	130.9
6.699	-14.530	88.75°	261.75°	4.75°	- 40.5	130.7
7.818	-13.960	88.00°	260.25°	5.75°	- 31.3	131.2
9.906	-12.565	86.00°	258.00°	8.00°	- 15.8	131.6
11.749	-10.861	84.00°	255.25°	10.25°	- 5.5	132.0
13.304	- 8.890	81.75°	252.00°	13.00°	7.8	132.9
14.530	- 6.699	78.75°	248.25°	16.50°	22.3	133.6
15.400	- 4.342	76.00°	243.75°	20.25°	34.0	135.2
15.890	- 1.880	72.00°	238.00°	25.00°	45.6	136.9
16.285	- 1.010	70.25°	235.25°	27.25°	49.6	137.9
16.285	1.010	66.00°	227.50°	33.25°	60.3	141.6
15.890	1.880	61.00°	218.75°	40.00°	72.1	146.7
16.220	2.500	49.00°	196.00°	56.50°	89.2	166.0
15.693	3.122	11.00°	137.00°	106.00°	122.2	---
15.400	4.342	358.50°	122.00°	119.75°	129.2	46.0
15.011	5.538	351.25°	115.25°	127.00°	132.1	60.1
14.530	6.699	347.75°	109.75°	131.25°	133.1	64.2
13.304	8.890	337.75°	103.00°	139.75°	135.0	75.2
11.749	10.861	331.25°	96.75°	146.00°	135.1	79.4
9.906	12.565	325.25°	92.25°	151.25°	133.1	83.1
7.818	13.960	319.50°	87.00°	157.00°	131.5	85.4
5.538	15.011	312.25°	81.00°	163.25°	130.8	87.8
3.122	15.693	305.25°	74.25°	170.00°	132.1	89.0
1.880	15.890	301.75°	70.00°	174.25°	136.4	89.0

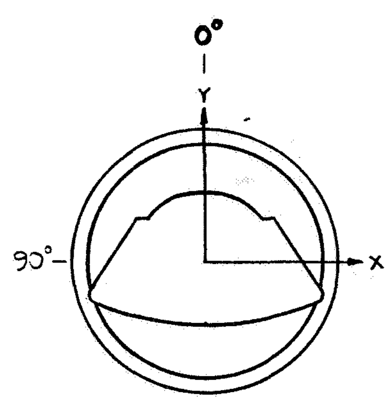

TABLE IV.- TEST DATA FOR EXTERNAL CONFIGURATION AT 7,500 POUNDS DISPLACEMENT

Test Data				Calculated Data		
Load Application Pt.		Waterline Intersect Points on Ring		Heel Angle, Degrees	Buoyancy Force and Centerline Intersection Sta. In.	Waterline and Centerline Intersection Sta. In.
X, In.	Y, In.	Load Side	Other Side			
1.880	-15.890	91.0°	266.0°	1.50°	-68.0	129.0
3.122	-15.693	90.0°	265.0°	2.50°	-50.4	129.1
4.342	-15.400	89.5	263.5°	3.50°	-40.4	130.0
5.538	-15.011	88.0°	262.0°	5.00°	-23.0	130.0
6.699	-14.530	87.0°	261.0°	6.00°	-19.9	130.0
7.818	-13.960	85.5°	260.0°	7.25°	-13.9	129.5
9.906	-12.565	83.0	256.5°	10.20°	4.5	130.4
11.749	-10.861	80.0°	253.0°	13.50°	17.3	130.9
13.304	- 8.890	77.0°	248.5°	17.25°	29.3	132.0
14.530	- 6.699	73.0°	243.0°	22.00°	42.1	133.4
15.400	- 4.342	68.0°	235.5°	28.25°	55.8	135.9
15.890	- 1.880	61.5°	224.5°	37.00°	69.6	140.9
16.285	1.010	44.5°	192.0°	61.75°	94.6	174.8
15.890	1.880	36.5°	180.5°	71.50°	100.9	206.2
15.693	3.122	18.0°	151.5°	95.25°	115.4	--
15.400	4.342	5.0°	134.5°	110.25°	123.2	22.0
15.011	5.538	356.0°	124.0°	120.00°	127.0	52.0
14.530	6.699	349.5°	116.5°	127.00°	131.0	63.5
13.304	8.890	339.5°	106.5°	137.50°	135.8	73.8
11.749	10.861	331.5°	100.0°	143.75°	134.0	79.8
9.906	12.565	325.0°	94.0°	150.50°	133.9	84.4
7.818	13.960	318.0°	89.0°	156.50°	131.7	87.8
5.538	15.011	311.0°	83.0°	163.00°	130.6	90.0
3.122	15.693	304.0°	76.0°	170.00°	130.6	91.0
1.880	15.890	300.0°	72.0°	174.00°	135.2	91.4

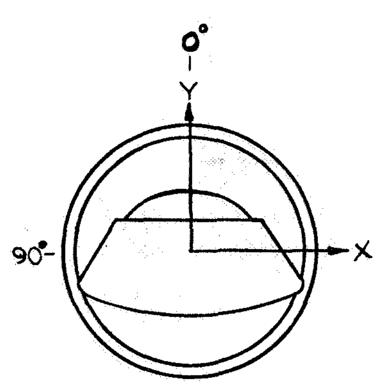

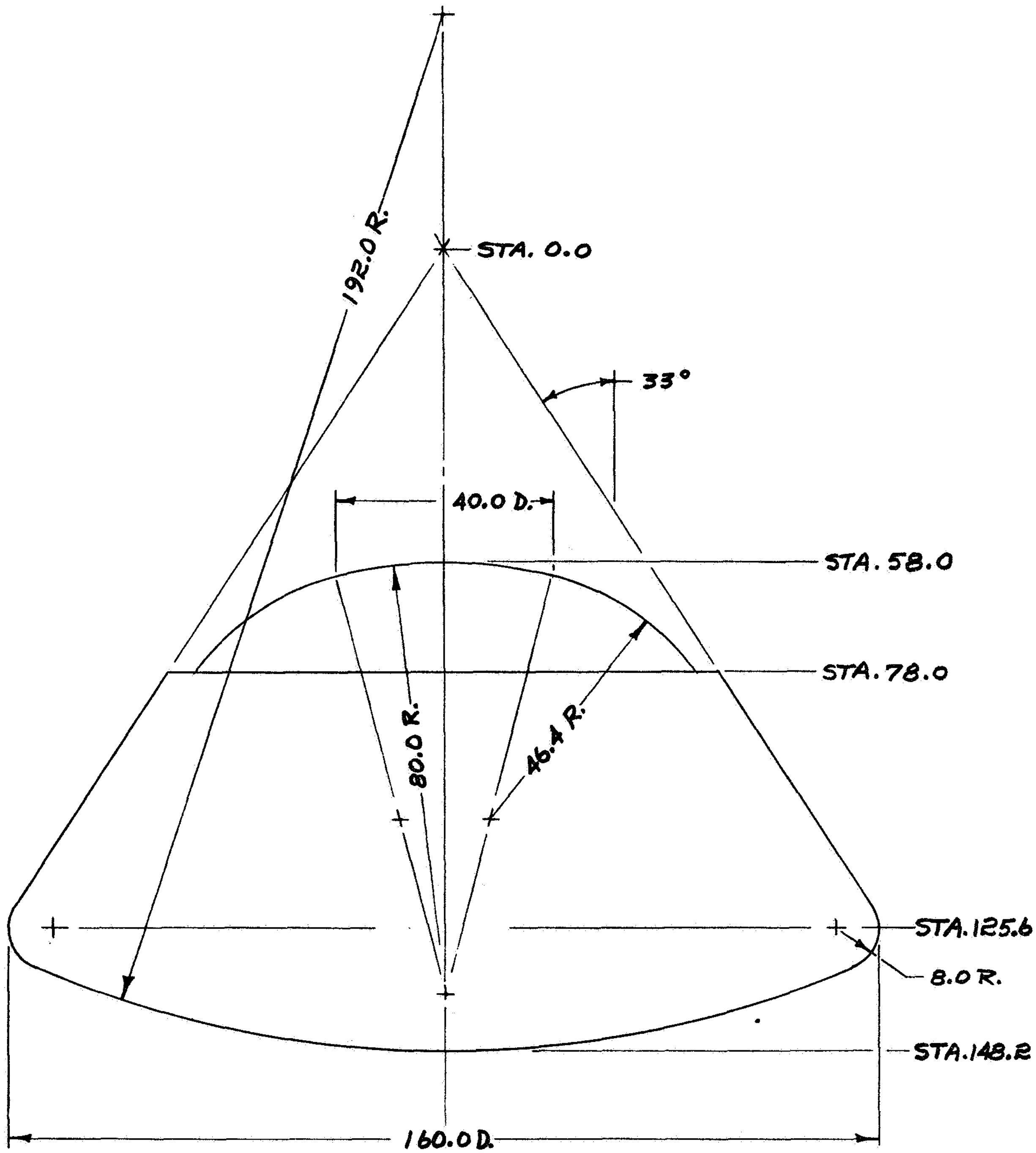

Figure 1.- Dimensions of External Shape
(Full Size)

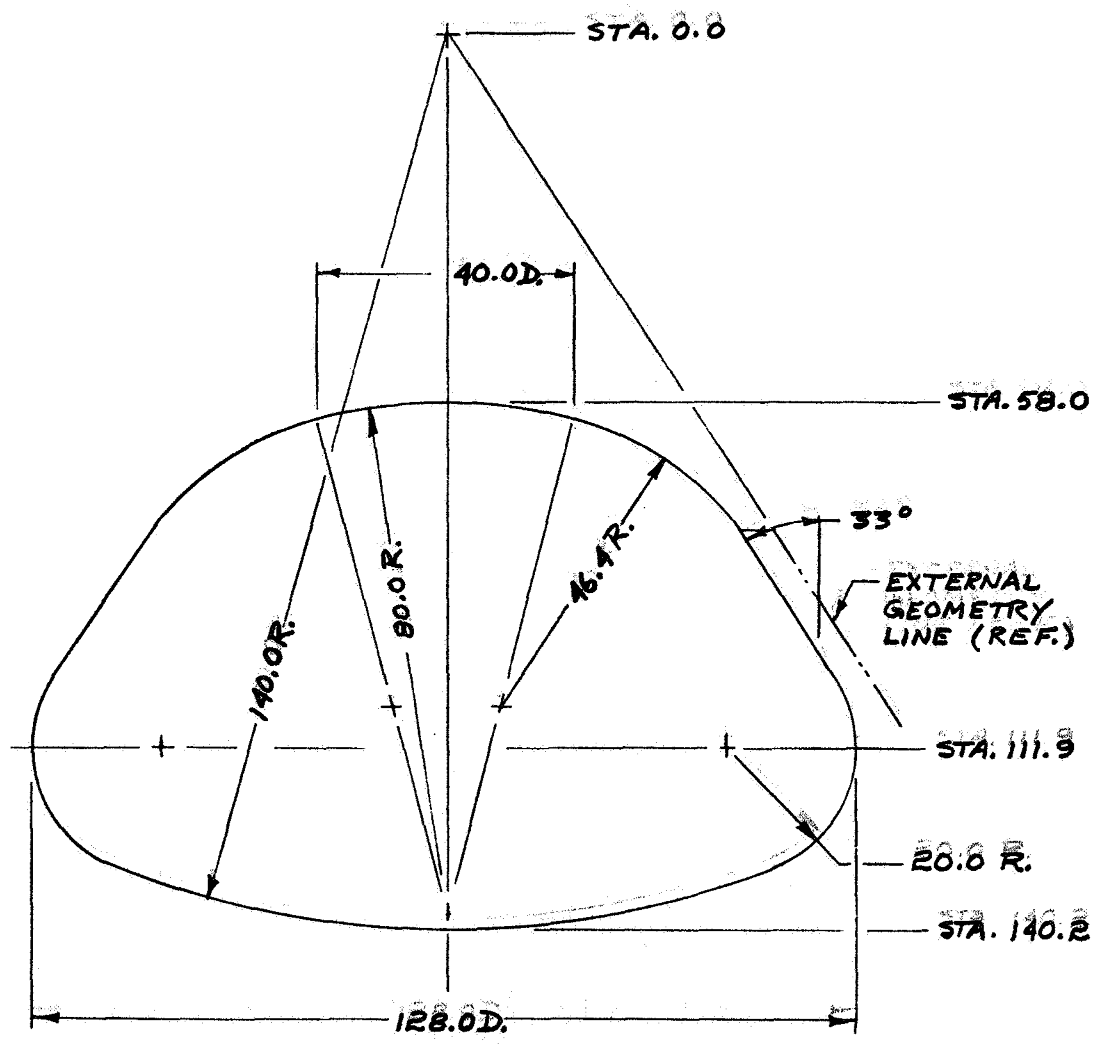

Figure 2.- Dimensions of Pressure Vessel
(Full Size)

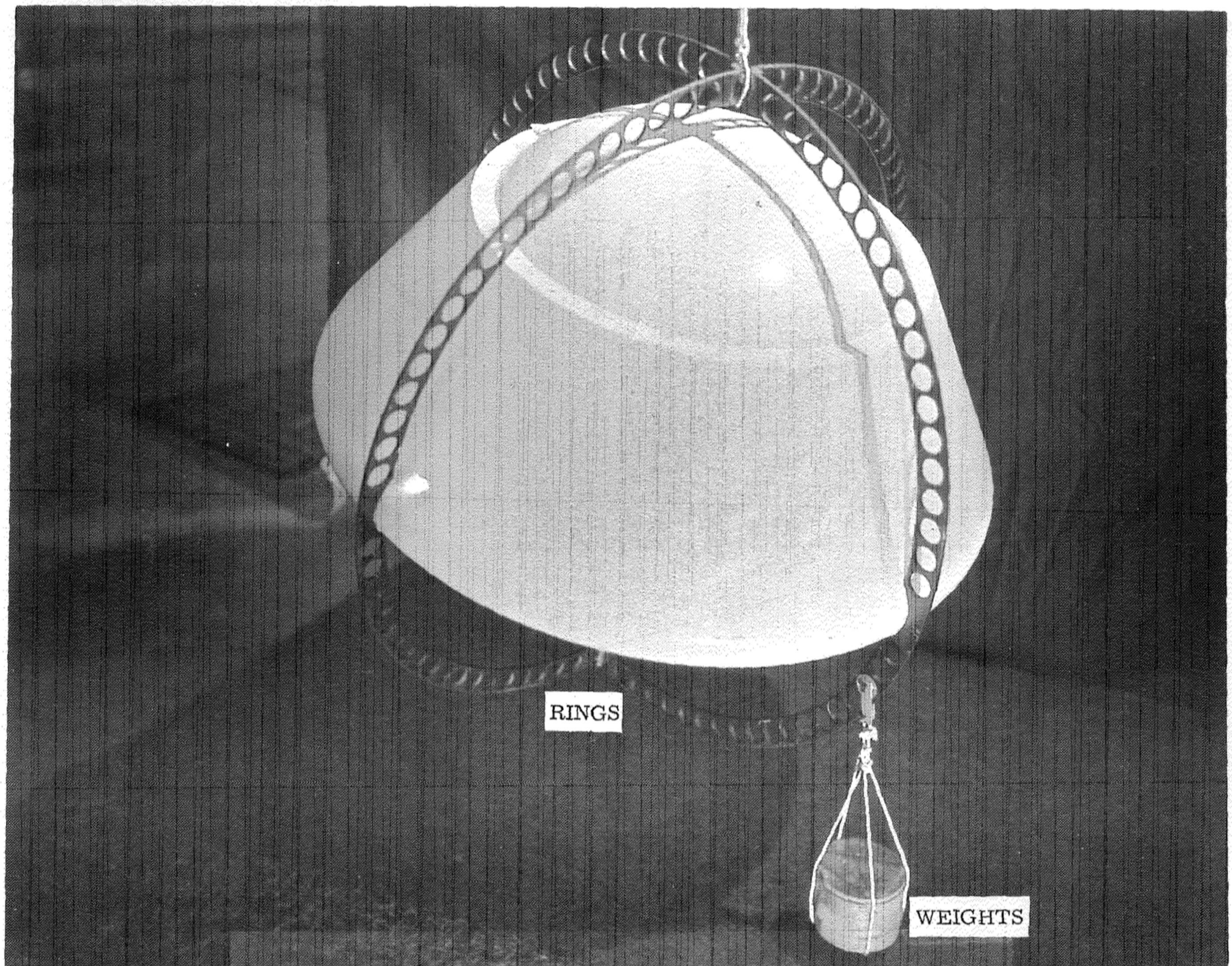

Figure 3.- External Geometry Model with
Ballasting Apparatus Attached

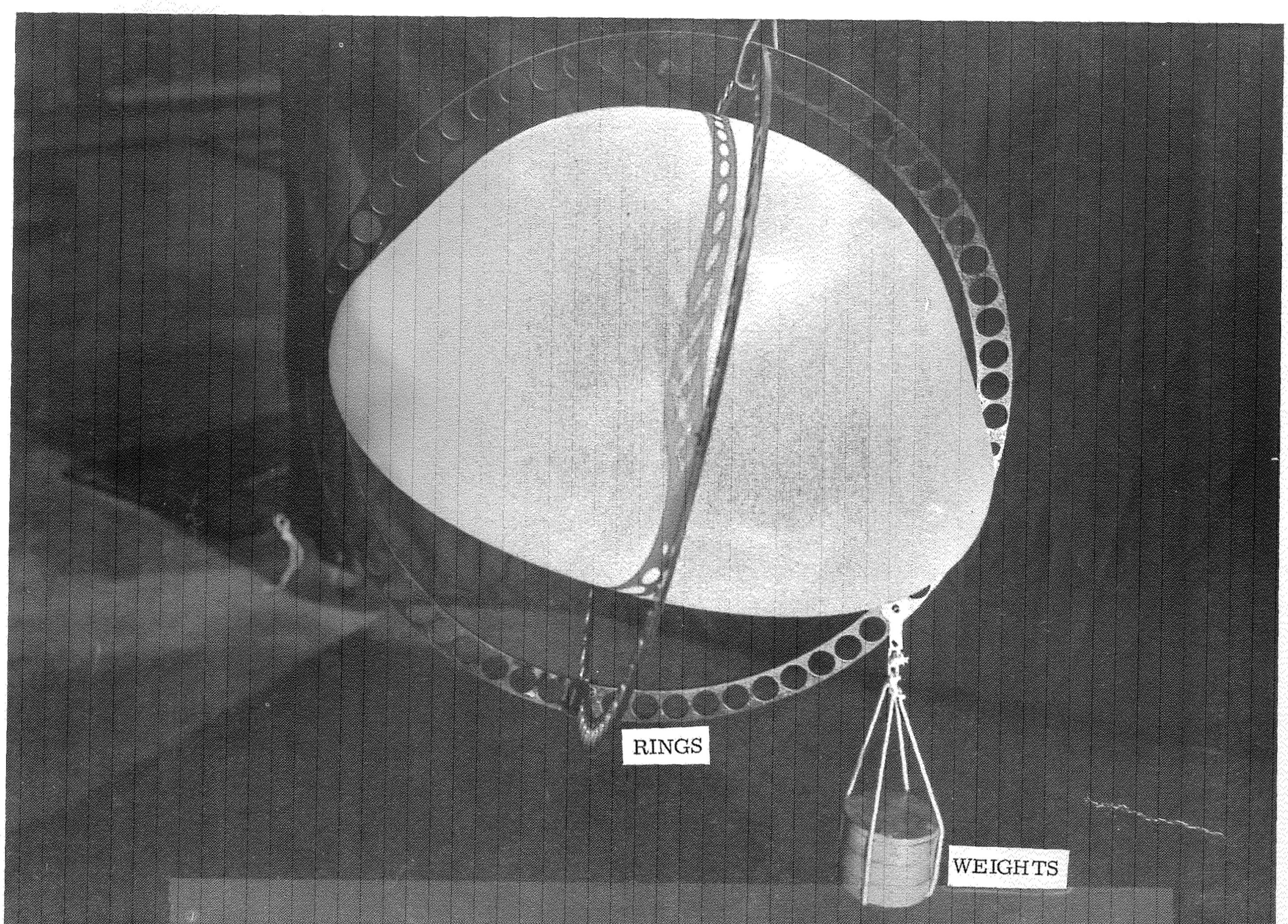

Figure 4.- Pressure Vessel Model with
Ballasting Apparatus Attached

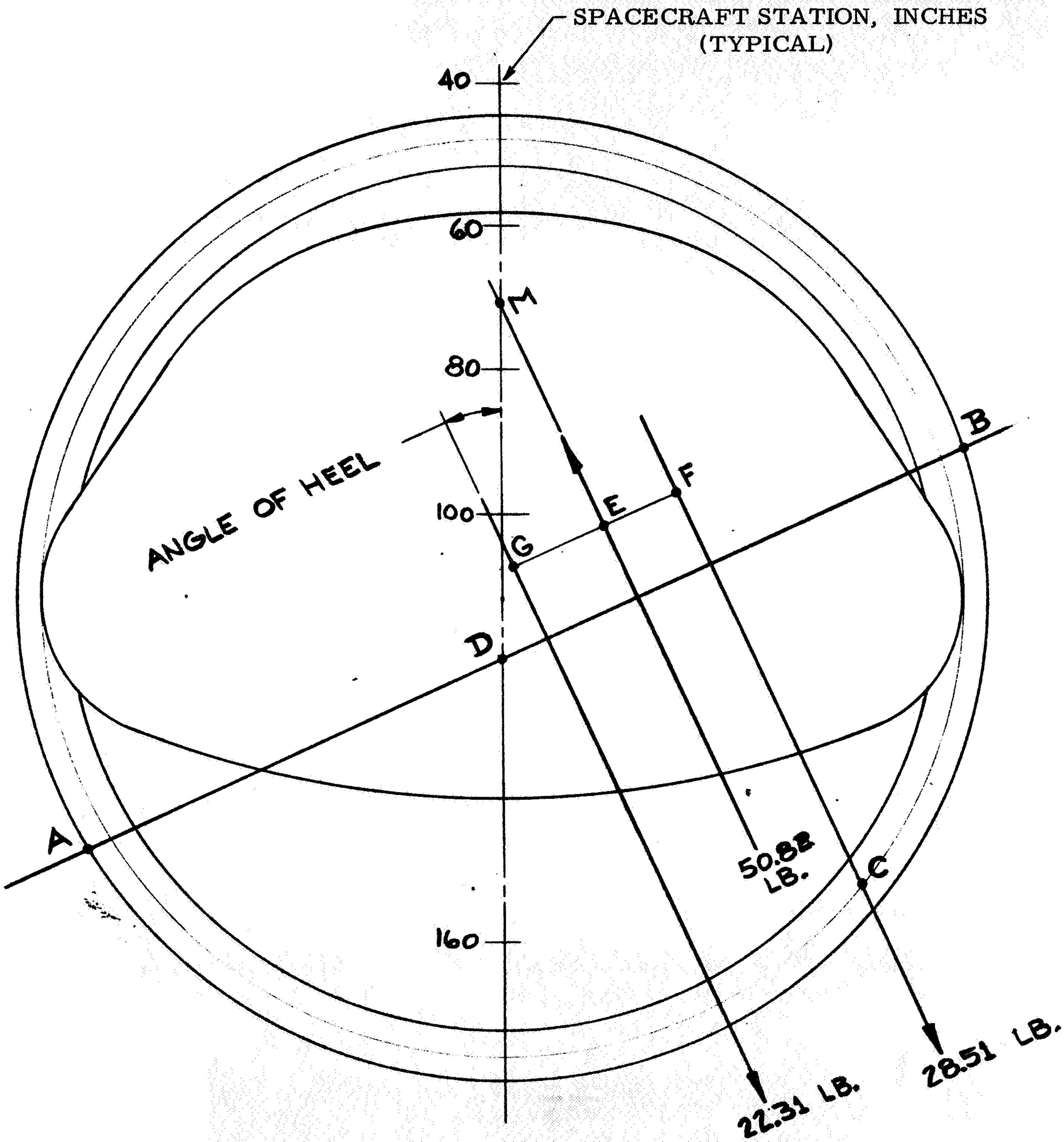

Figure 5.- Diagram of Forces on
Pressure Vessel Model

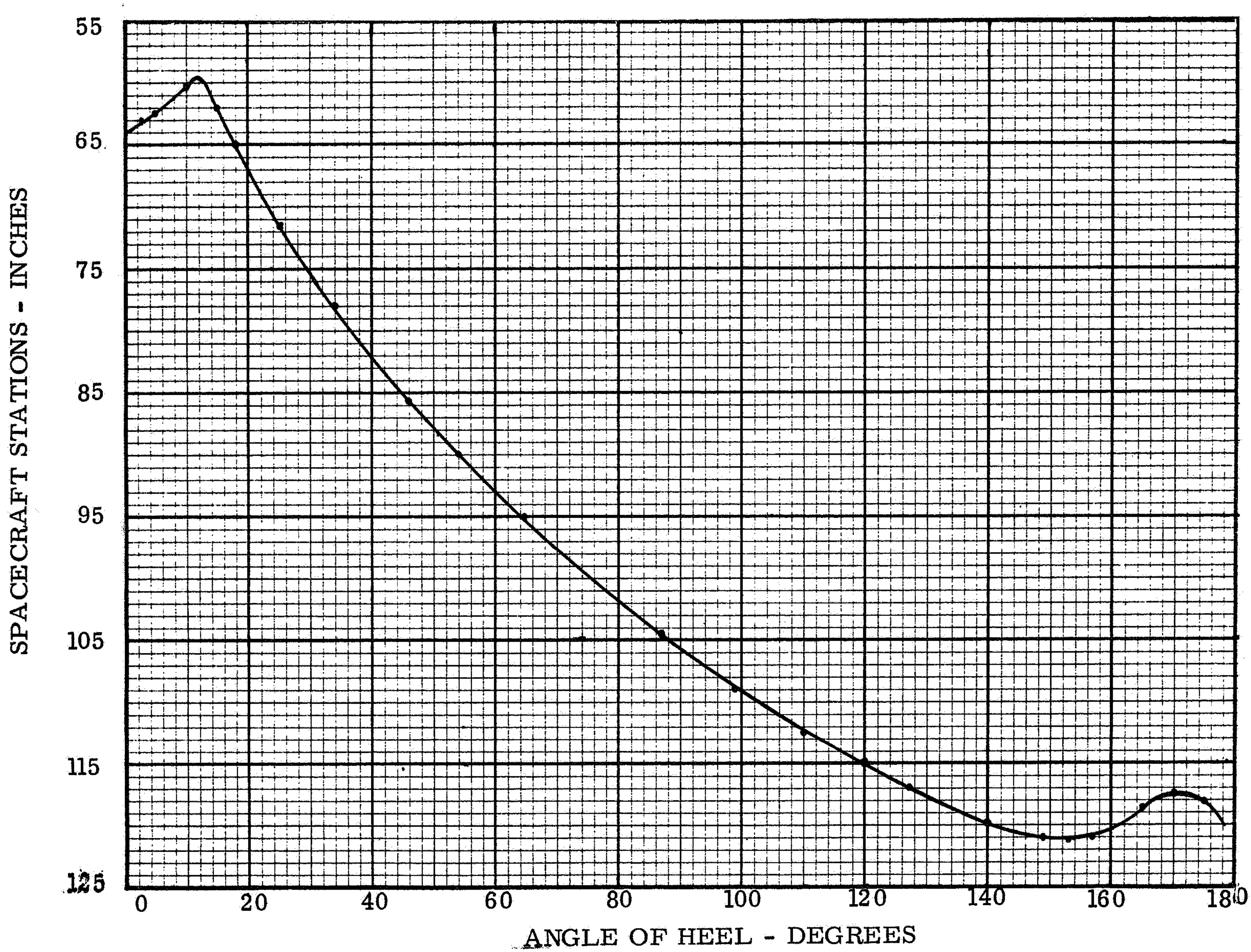

Figure 6.- Buoyancy Force Lines of Action Intersection with Vertical Centerline vs Angle of Heel for Pressure Vessel Model at 6,517 Pounds Displacement

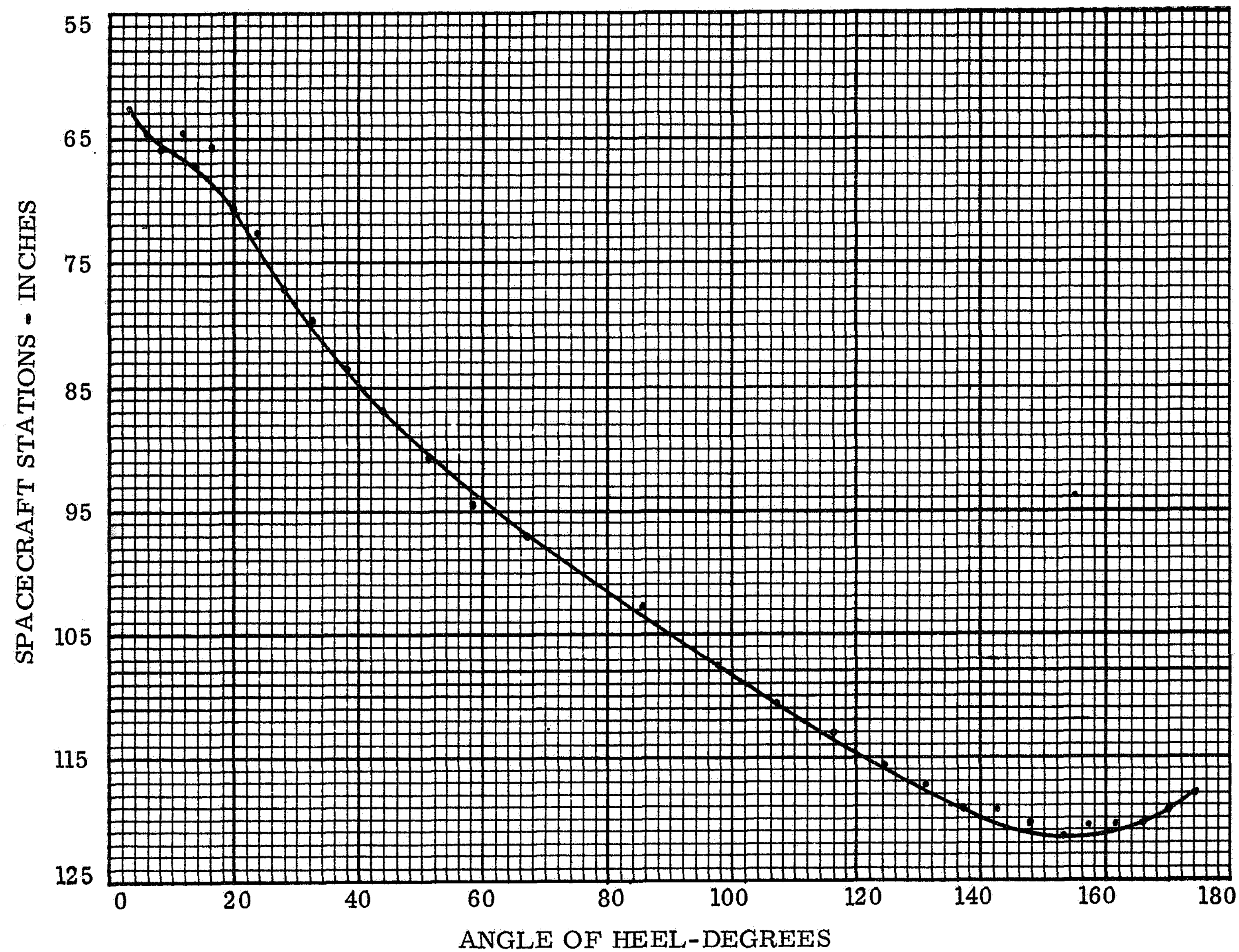

Figure 7.- Buoyancy Force Lines of Action Intersection with Vertical Centerline vs Angle of Heel for Pressure Vessel Model at 7,500 Pounds Displacement

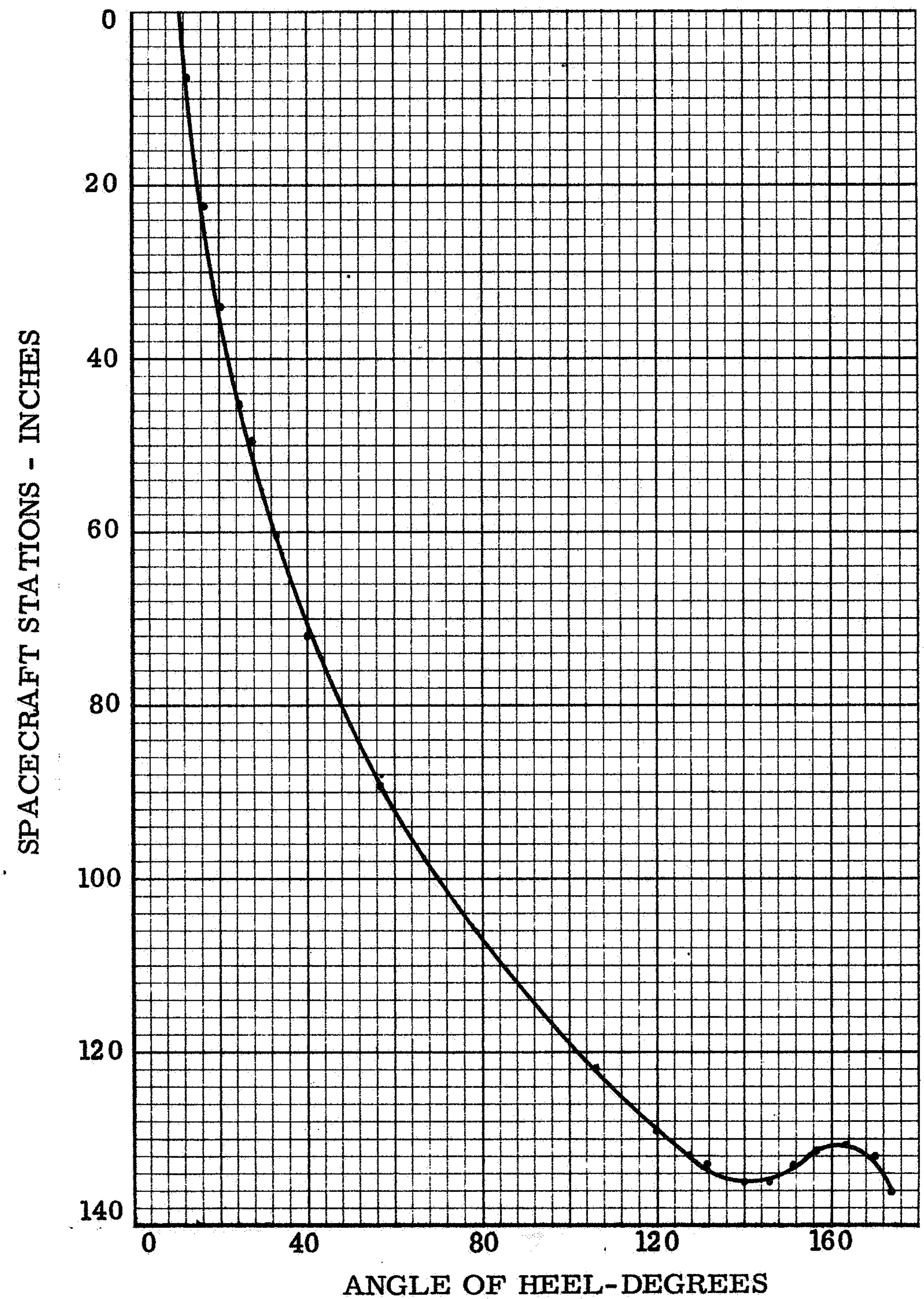

Figure 8.- Buoyancy Force Lines of Action Intersection with Vertical Centerline vs Angle of Heel for External Configuration Model at 6,517 Pounds Displacement

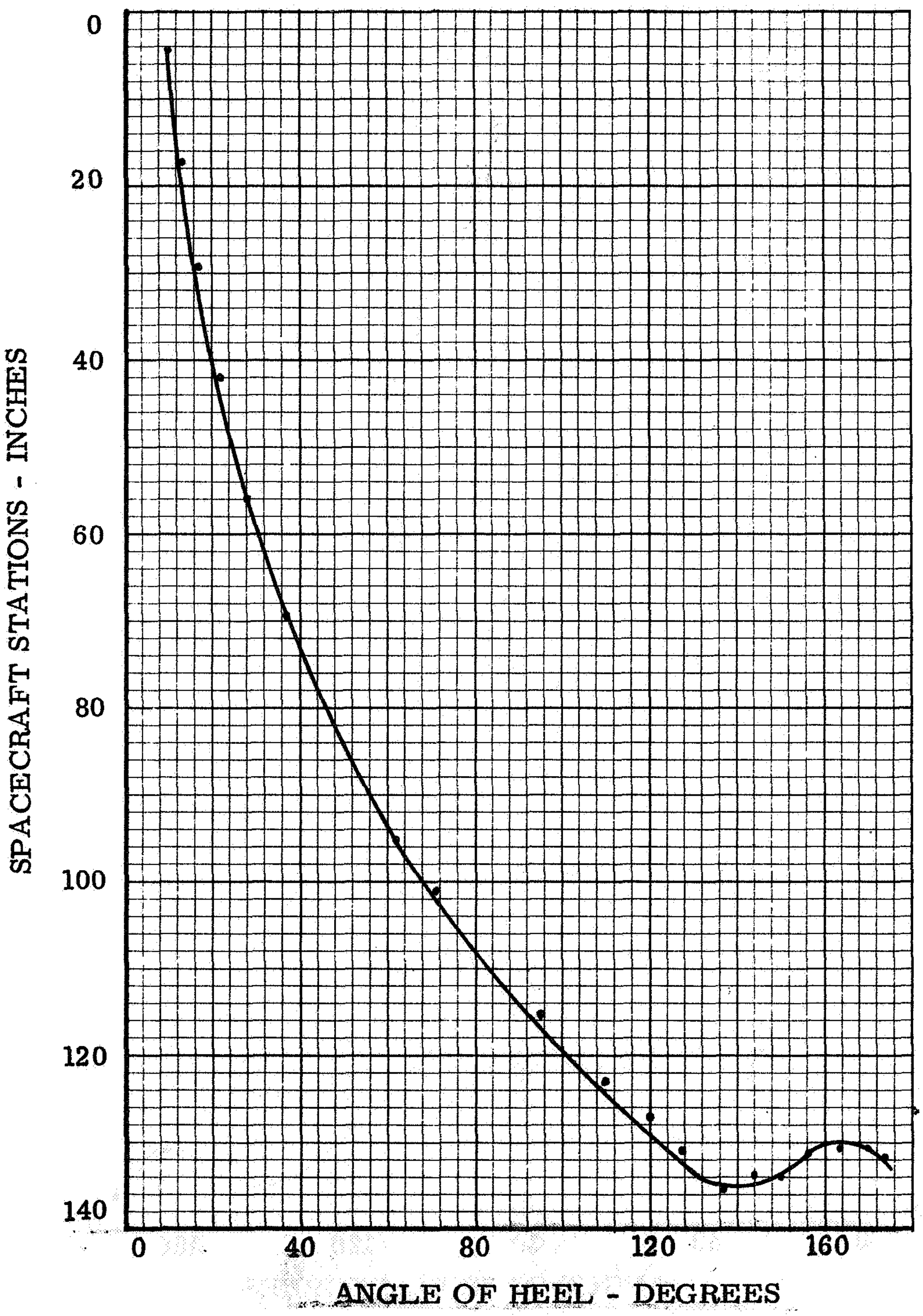

Figure 9.- Buoyancy Force Lines of Action Intersection with Vertical Centerline vs Angle of Heel for External Configuration Model at 7,500 Pounds Displacement

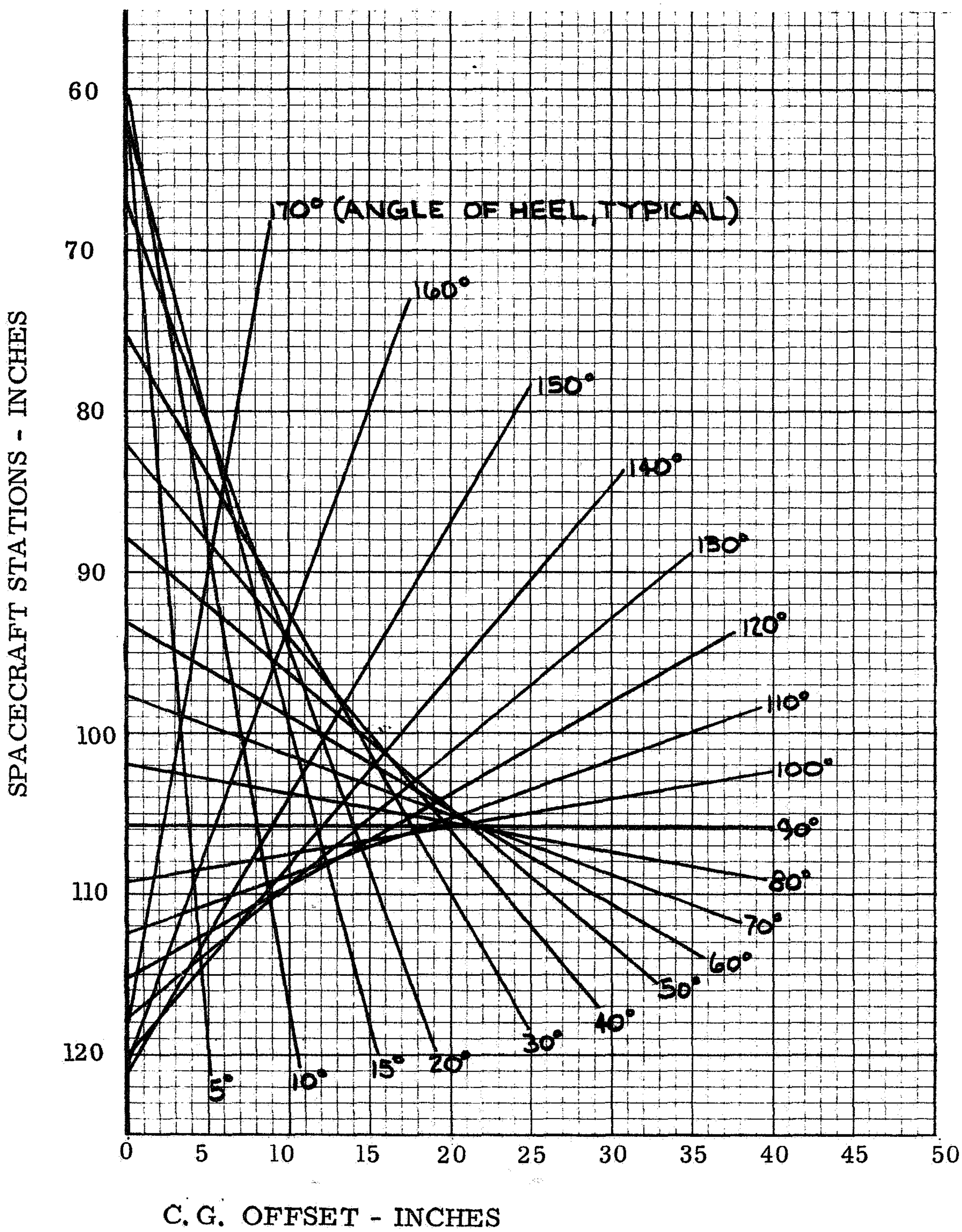

Figure 10.- Buoyancy Force Lines of Action for Pressure Vessel at 6,517 Pounds Displacement

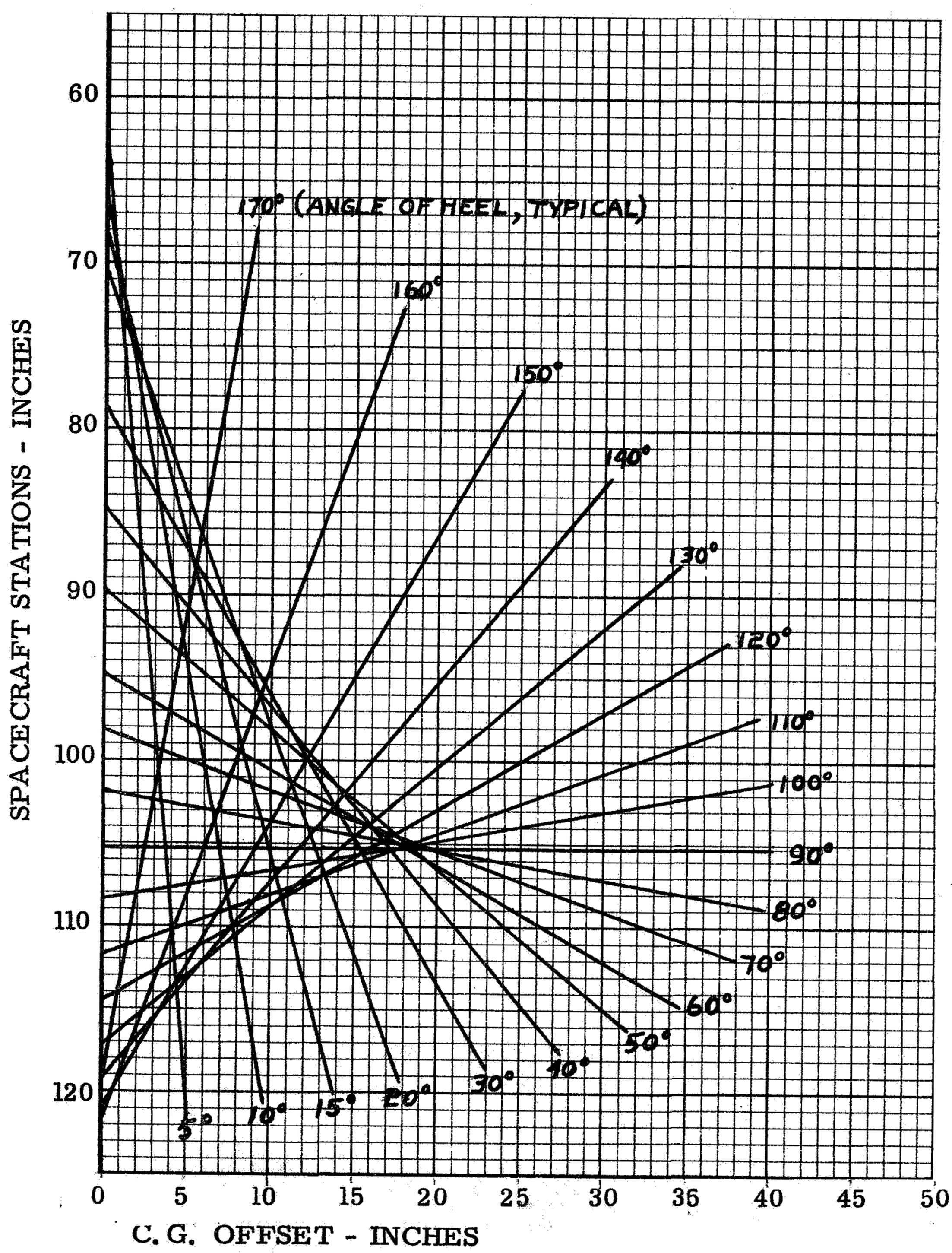

Figure 11.- Buoyancy Force Lines of Action for Pressure Vessel at 7,500 Pounds Displacement

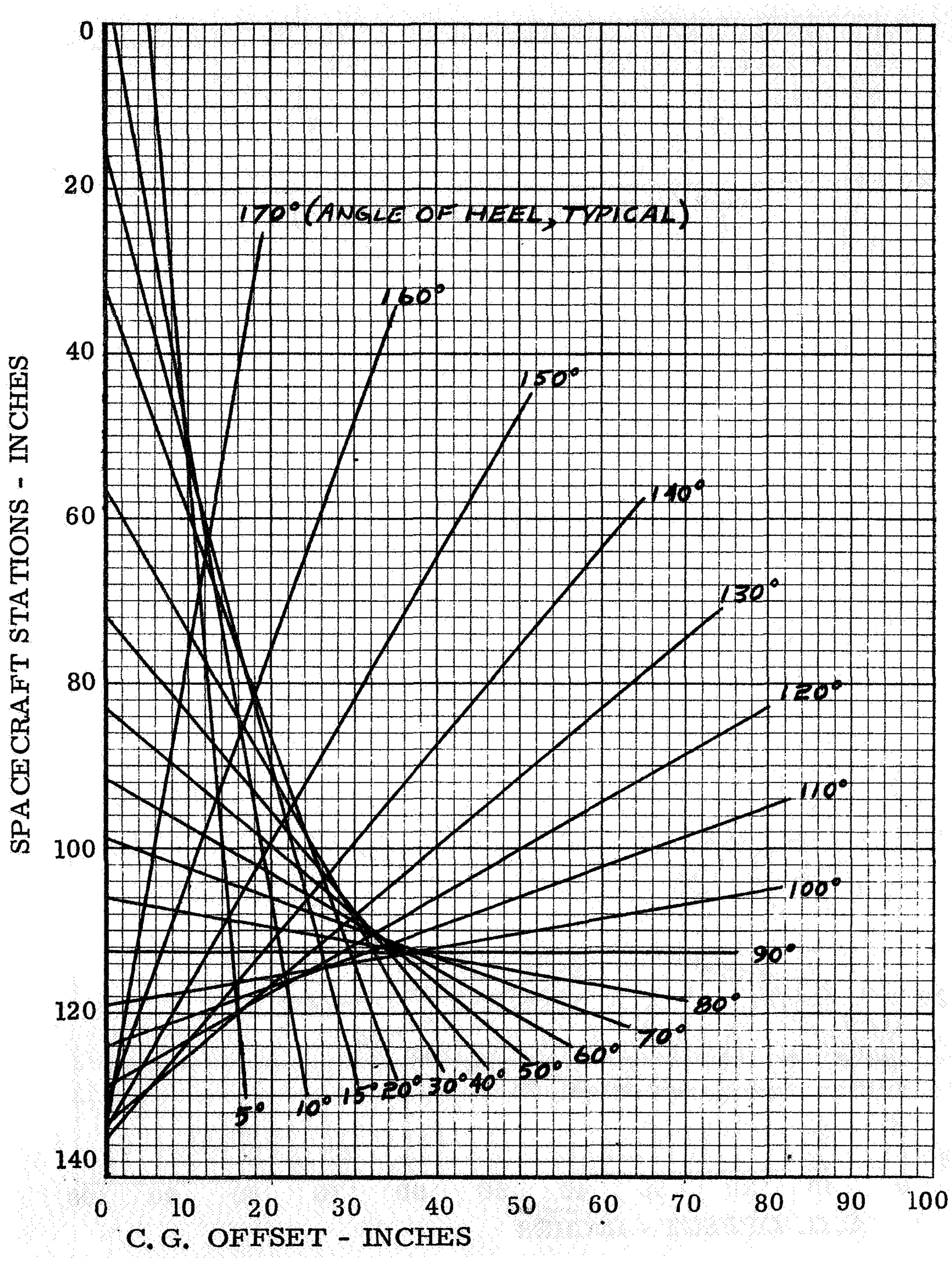

Figure 12.- Buoyancy Force Lines of Action for External Configuration at 6,517 Pounds Displacement

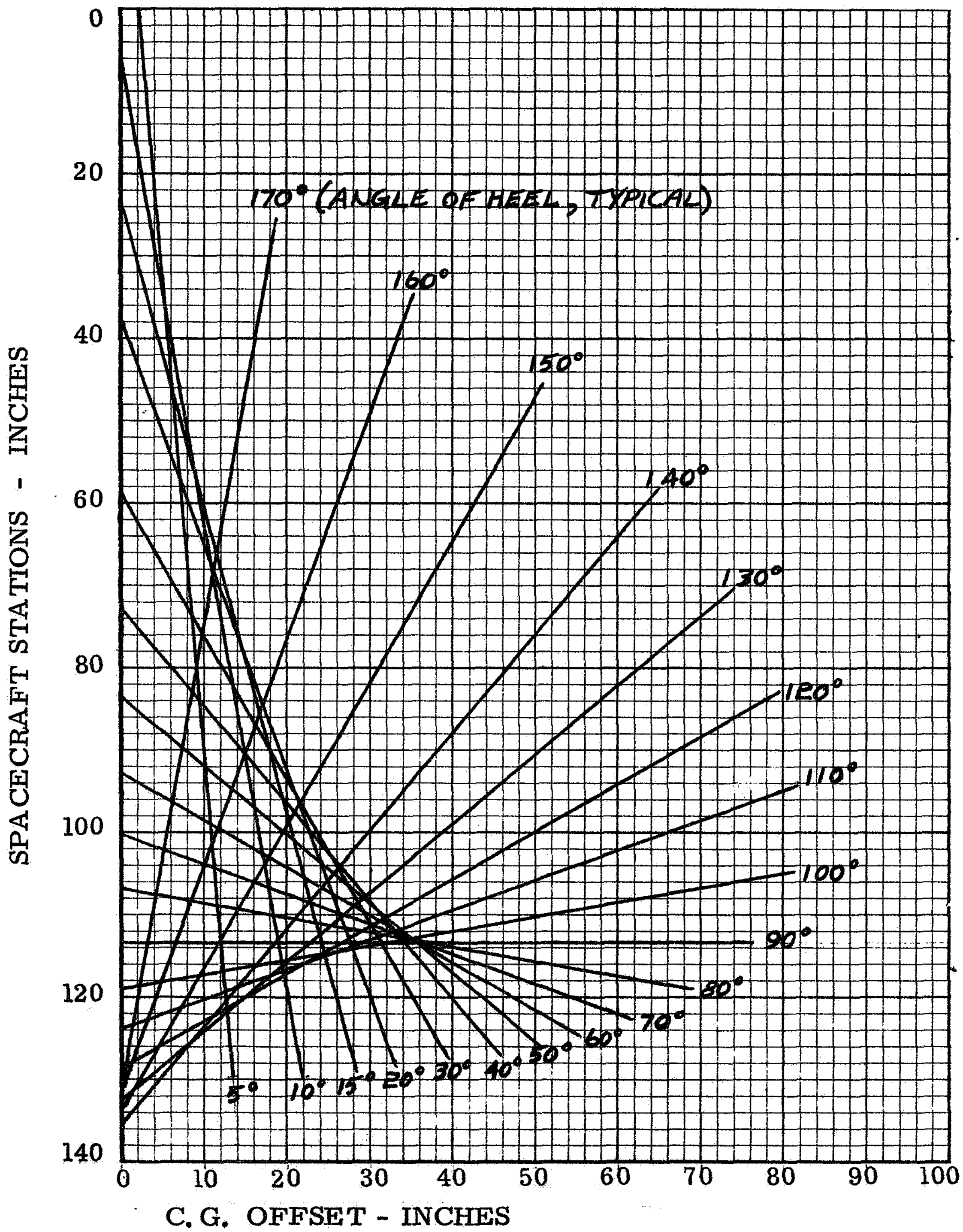

Figure 13.- Buoyancy Force Lines of Action for External Configuration at 7,500 Pounds Displacement

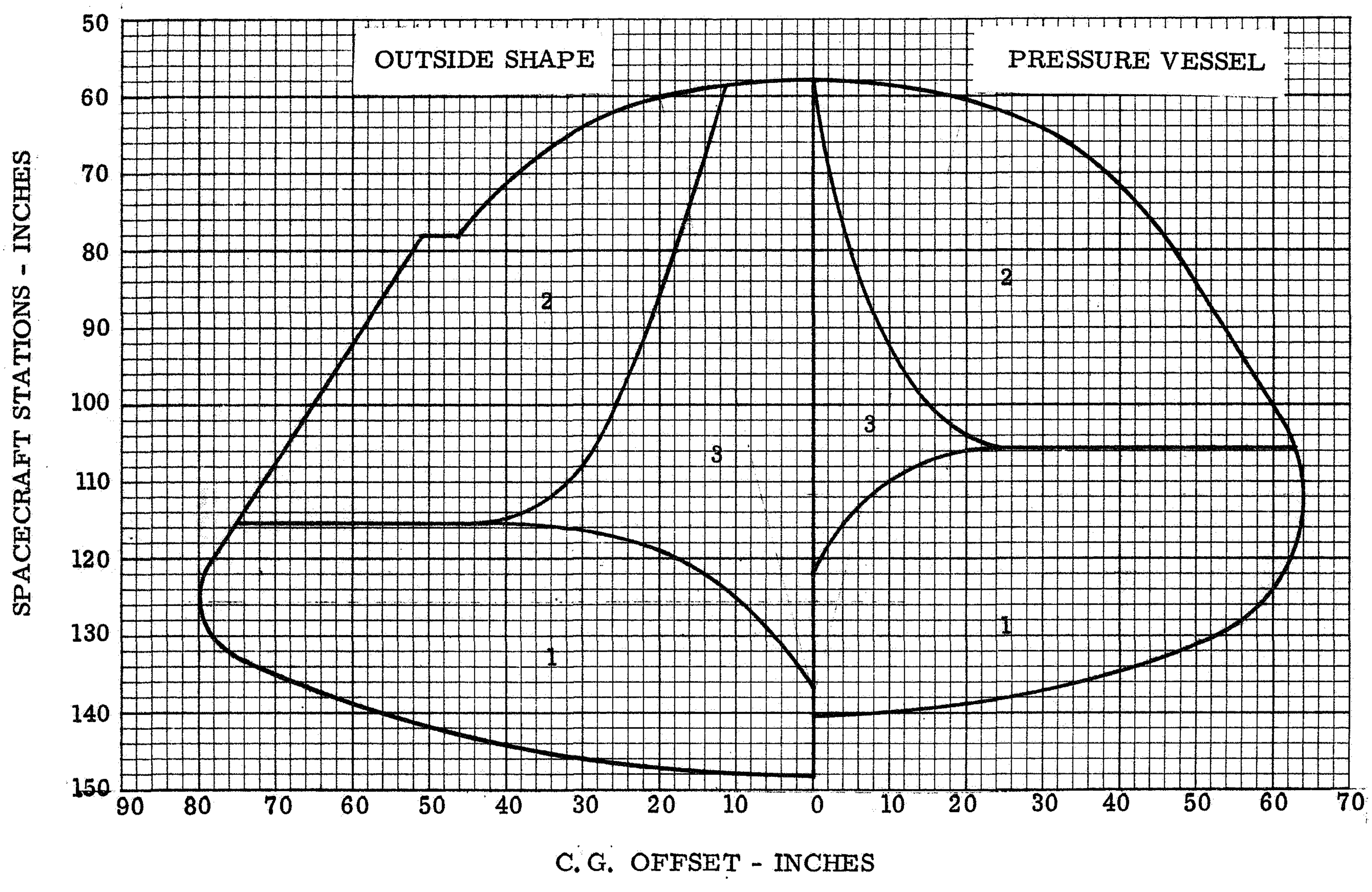

Figure 14.- Regions of Significant C.G. Locations for Pressure Vessel and External Configuration at 6,517 Pounds Displacement

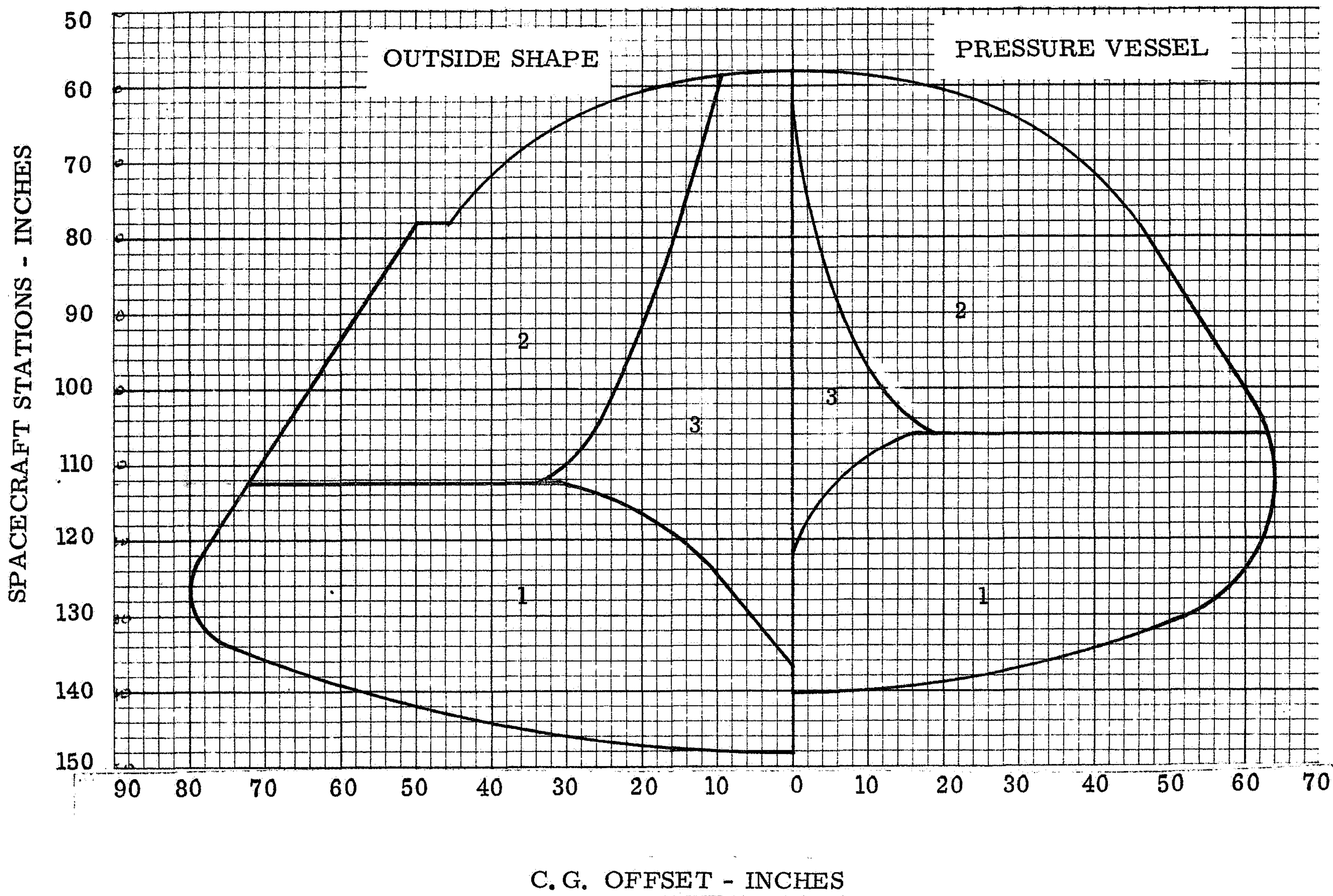

Figure 15.- Regions of Significant C.G. Locations for Pressure Vessel and External Configuration at 7,500 Pounds Displacement

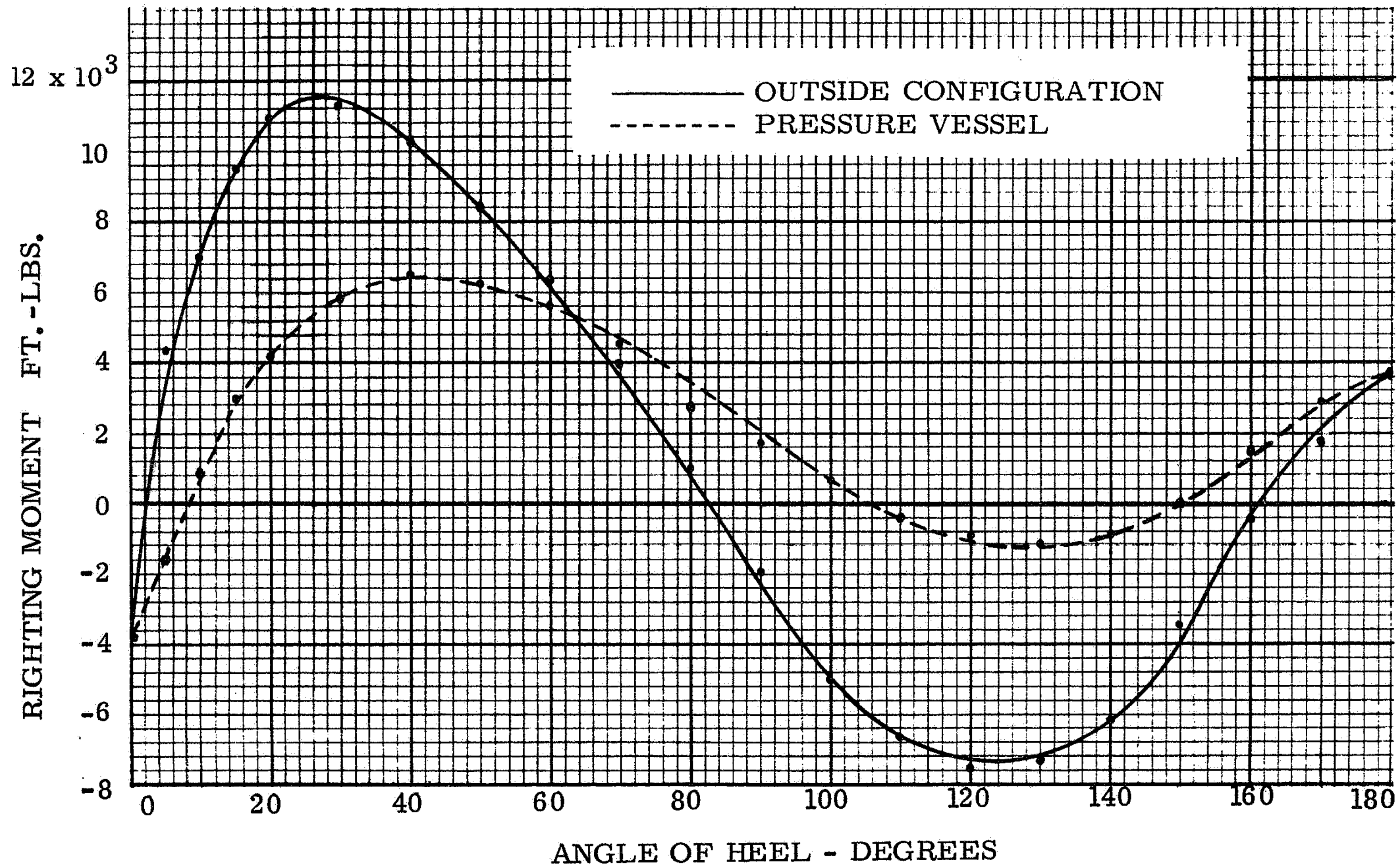

Figure 16.- Righting Moment vs Angle of Heel for Pressure Vessel and External Configuration at 6,517 Pounds Displacement with C.G. Located at Spacecraft Station 109.0, Offset 7.0 Inches

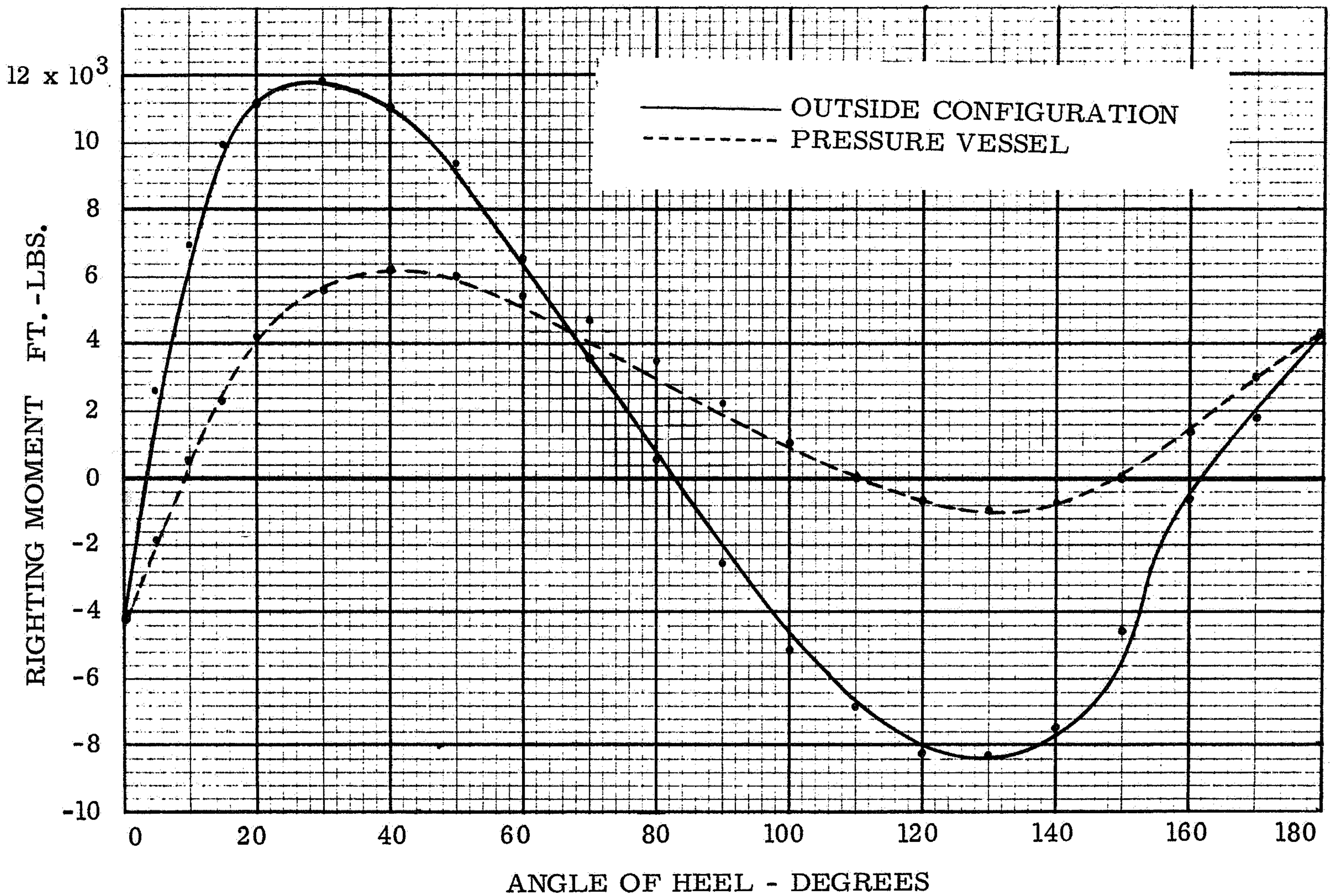

Figure 17.- Righting Moment vs Angle of Heel for Pressure Vessel and External Configuration at 7,500 Pounds Displacement with C.G. Located at Spacecraft Station 109.0, Offset 7.0 Inches

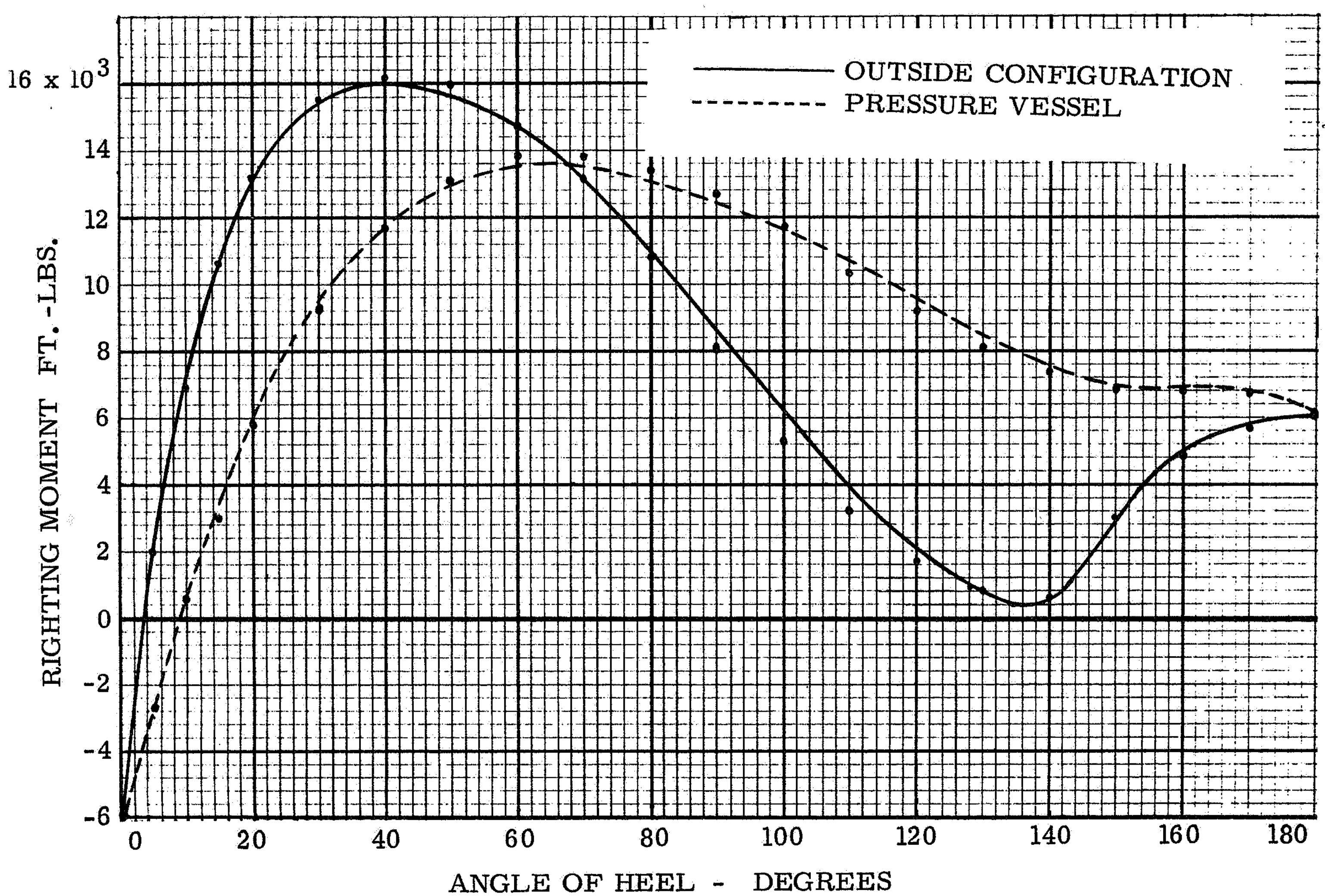

Figure 18.- Righting Moment vs Angle of Heel for Pressure Vessel and External Configuration at 7,500 Pounds Displacement with C.G. Located at Spacecraft Station 126.0, Offset 10.0 Inches

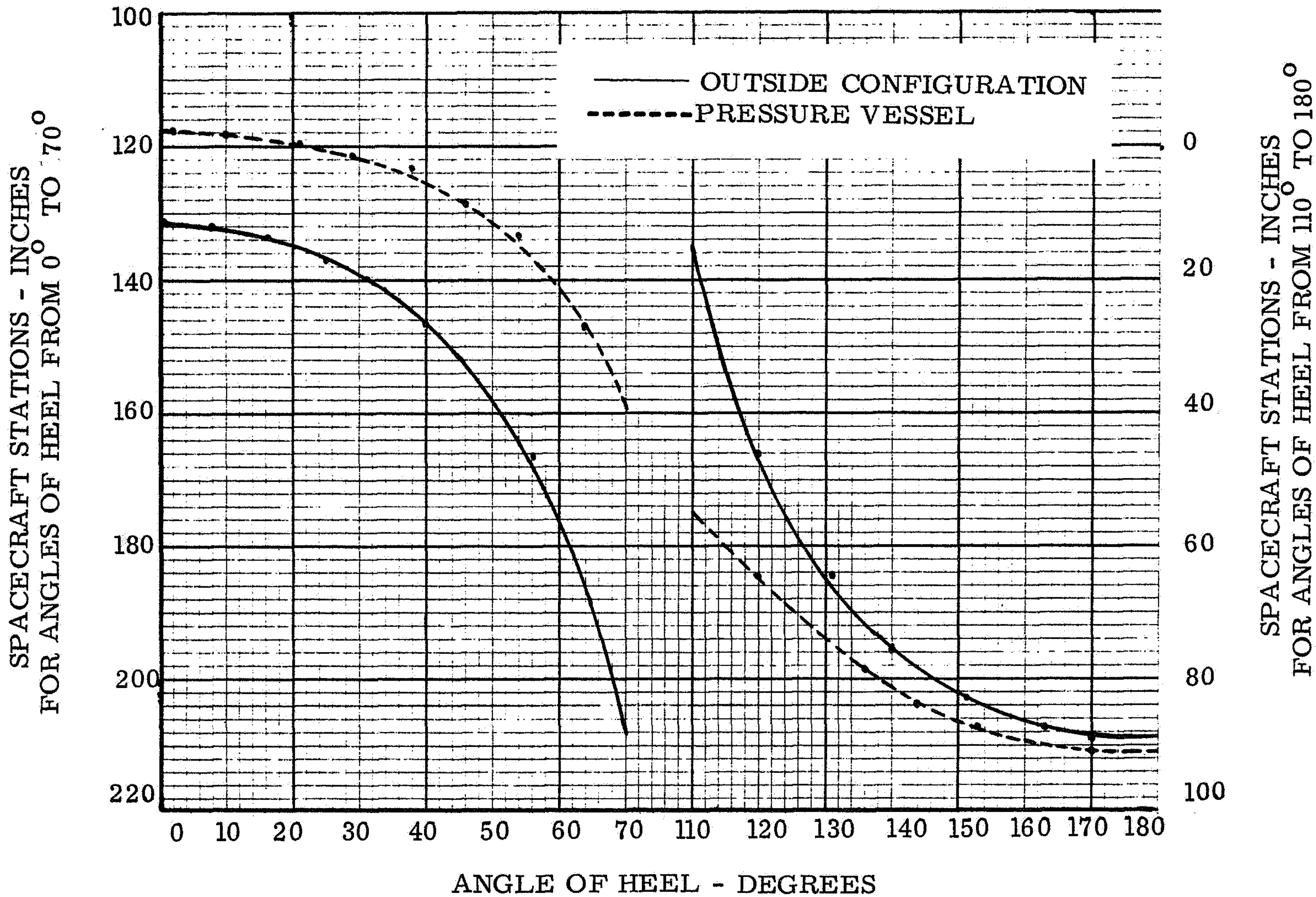

Figure 19.- Waterline and Spacecraft Centerline Intersection with Displacement of 6,517 Pounds

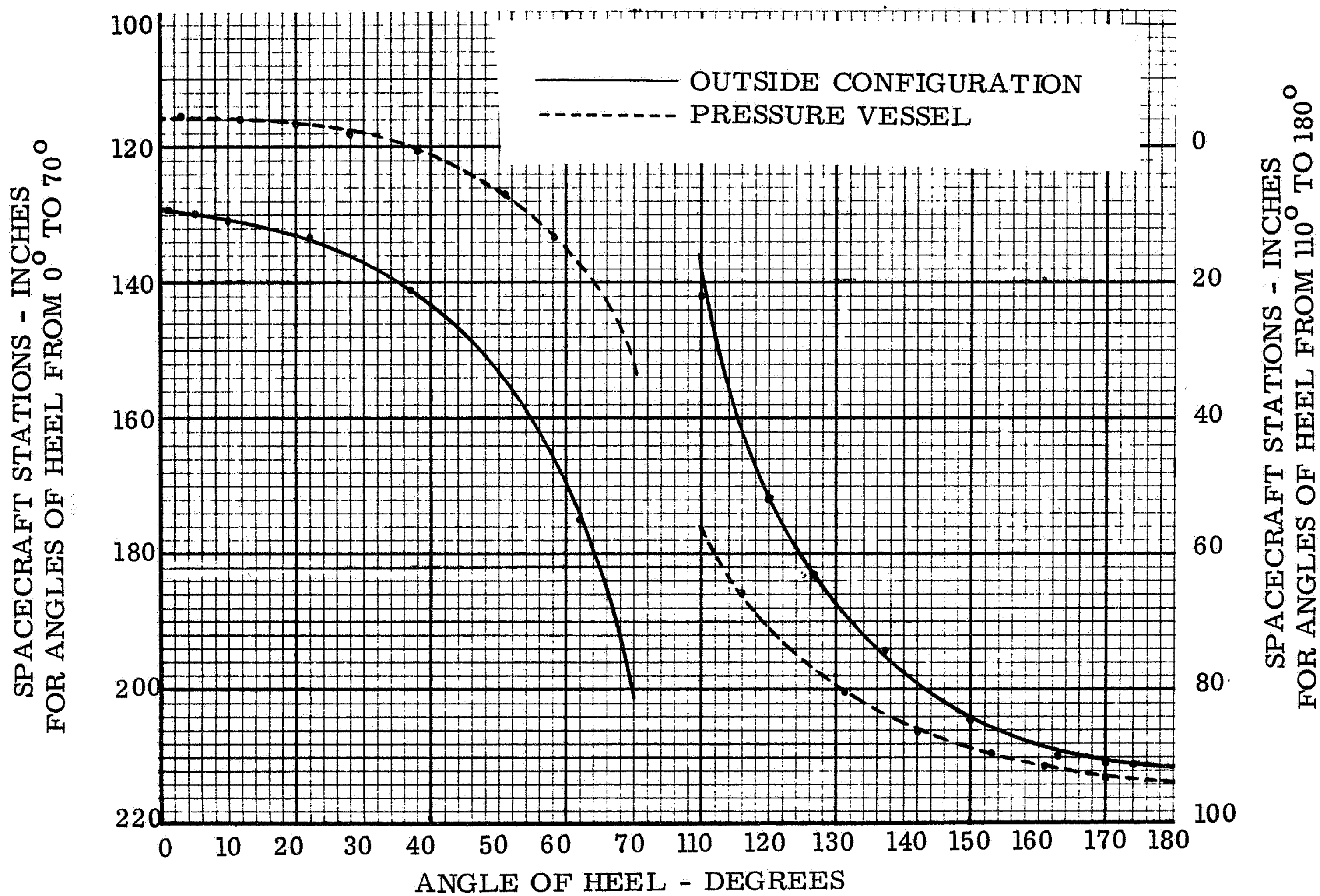

Figure 20.- Waterline and Spacecraft Centerline Intersection with Displacement of 7,500 Pounds

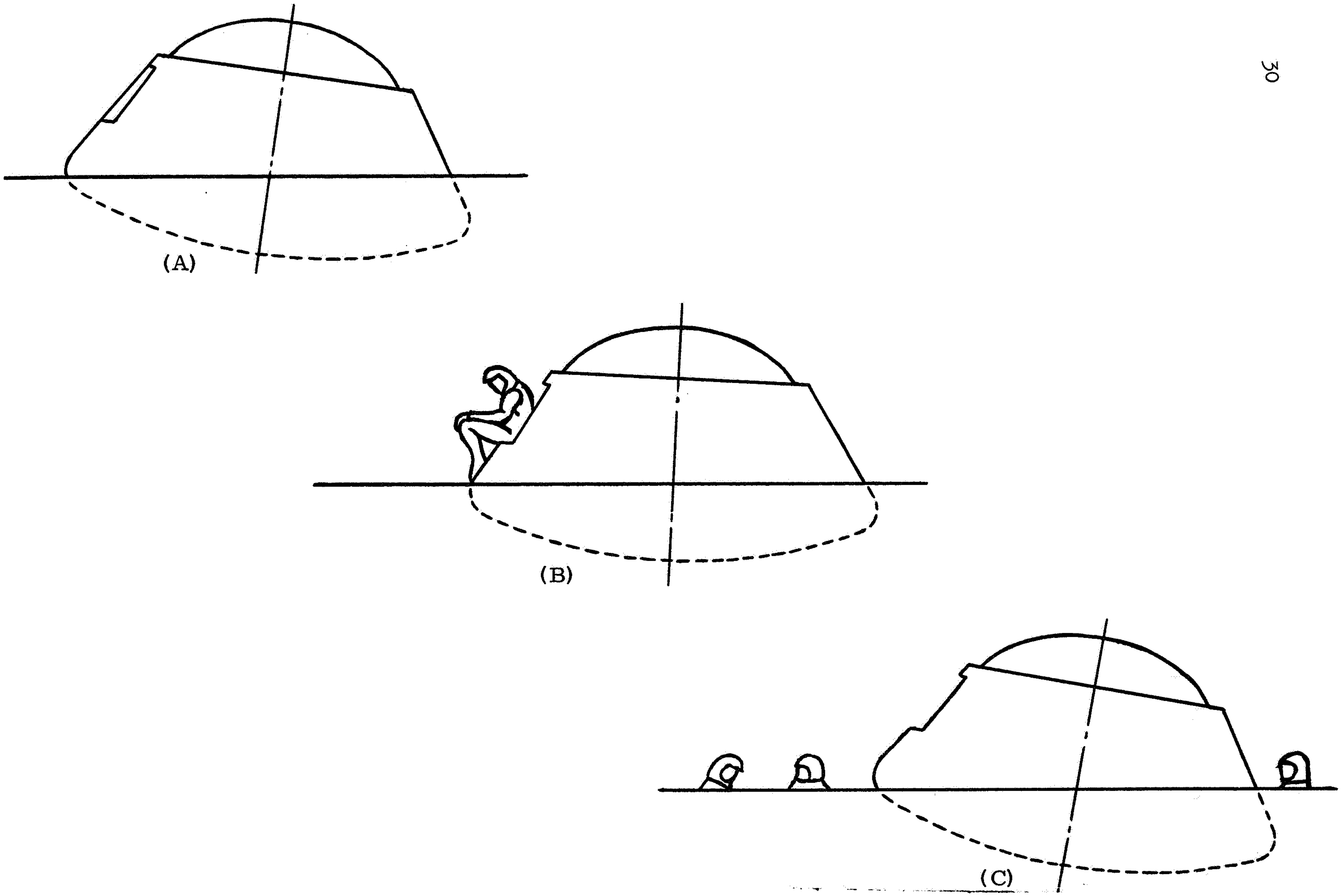

Figure 21.- Apollo Flotation Characteristics During Astronaut Egress-Spacecraft Upright

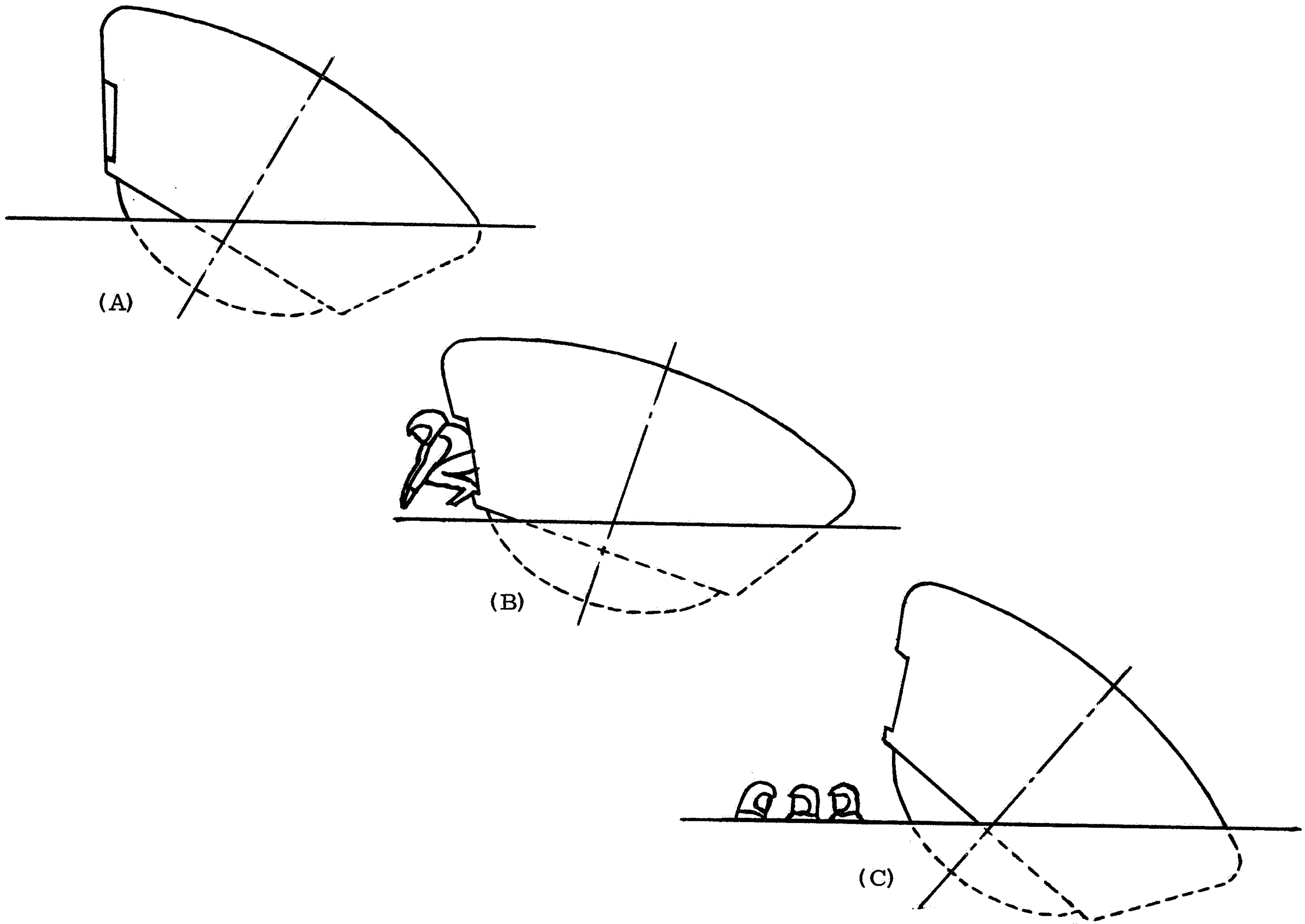

Figure 22.- Apollo Flotation Characteristics During Astronaut Egress-Spacecraft Inverted